Theoretical investigation of nonstatistical dynamics, energy transfer, and intramolecular vibrational relaxation in isomerization reactions of matrixisolated HONO/Xe

Paras M. Agrawal, Donald L. Thompson, and Lionel M. Raff

Citation: The Journal of Chemical Physics **101**, 9937 (1994); doi: 10.1063/1.467895
View online: http://dx.doi.org/10.1063/1.467895
View Table of Contents: http://scitation.aip.org/content/aip/journal/jcp/101/11?ver=pdfcov
Published by the AIP Publishing

Theoretical investigation of nonstatistical dynamics, energy transfer, and intramolecular vibrational relaxation in isomerization reactions of matrix-isolated HONO/Xe

Paras M. Agrawal, Donald L. Thompson, and Lionel M. Raff
Department of Chemistry, Oklahoma State University, Stillwater, Oklahoma 74078

(Received 26 July 1994; accepted 18 August 1994)

Theoretical molecular dynamics studies of *cis–trans* isomerization, intramolecular vibration relaxation (IVR), and vibrational relaxation rates to lattice phonon modes of HONO isolated in a face-centered cubic (fcc) xenon matrix at 12 K are reported. The effect of the matrix environment upon the dynamics is obtained by comparison with the corresponding gas-phase results. Questions related to statistical vs nonstatistical behavior and the effect of lattice imperfections are also addressed. It is found that both $cis \rightarrow trans$ and $trans \rightarrow cis$ isomerization rates are significantly enhanced by the presence of the matrix in spite of the steric effects produced by the environment. It is shown that this result occurs because the matrix opens a (vibration→lattice phonon modes→rotation→torsional vibration) energy transfer path. The calculated isomerization rate coefficients indicate significant nonstatistical dynamics. The IVR rates in the matrix and in the gas phase are slow relative to the isomerization rates. Consequently, the isomerization cannot be statistical. The calculated $cis \rightarrow trans$ and $trans \rightarrow cis$ ratio is found to be significantly less than previously reported measurements indicate. Vibrational relaxation rates to the lattice phonon modes are found to be almost independent of the initial energy partitioning. It is suggested that this may be a result of the transfer rates approaching their limiting values determined by the Debye frequency of the lattice. The presence of lattice vacancies is found to exert a profound influence upon the dynamics. When the percentage of lattice vacancies approaches 20%, the calculated dynamics in the matrix are found to approach the gas-phase results. © *1994 American Institute of Physics.*

I. INTRODUCTION

Since their inception, matrix-isolation methods have been applied to an increasing range of chemical and physical problems.[1] Advances in this area have been described in review articles,[2,3] and recent experimental and theoretical papers[4–11] show that the study of the interaction of high-energy and high-intensity radiation with molecules, chemical reactions, intramolecular energy transfer, and cluster dynamics has been significantly advanced by the use of matrix-isolation techniques.

We have reported a series of theoretical studies[12–17] of intramolecular energy transfer and *cis–trans* isomerization of HONO in the gas-phase. Experimental investigations of the intramolecular dynamics of HONO under matrix-isolation conditions have also been reported.[18–20] In this paper, we report the results of theoretical molecular dynamics studies of *cis–trans* isomerization, intramolecular vibration relaxation (IVR), and vibrational relaxation rates to lattice phonon modes of HONO isolated in a face-centered cubic (fcc) xenon matrix at 12 K. Specifically, we determine the effect of the matrix environment upon the isomerization rates by comparison with previously reported gas-phase results.[16] In the gas phase, the isomerization rate has been found to depend upon the internal mode excited.[16] Such mode specific rate enhancement has also been reported for several systems under matrix isolation conditions.[18–20] The present paper explores the extent to which such effects are present in the HONO/Xe system. The effect of lattice vacancies have also been investigated.

The matrix model and potential-energy surface are described in Sec. II. The numerical methods and results are given and discussed in Sec. III. All results and conclusions are summarized in the final section.

II. MATRIX MODEL AND POTENTIAL-ENERGY SURFACE

The rare-gas matrix employed in the present study is the same as that used in our earlier investigation of matrix-isolated 1,2-difluoroethane.[11] It is a fcc lattice consisting of 125 unit cells arranged in a (5×5×5) structure. This model contains 14 atoms in each unit cell and 666 total lattice atoms, N. The effect of lattice vacancies have been investigated by the random removal of 10%–20% of the lattice atoms. HONO is assumed to be held interstitially such that its center of mass coincides with the center of the innermost unit cell of the (5×5×5) lattice.

The total potential, V, is taken to be the sum of three terms,

$$V = V_m + V_i + V_h. \tag{1}$$

Here, V_m is the potential for the rare gas–rare gas interaction, V_h is the intramolecular potential of HONO in the absence of the matrix, and V_i gives the interaction between the atoms of HONO and those of the lattice. V_m is assumed to have pairwise form,

$$V_m = \sum_{i<j}^{N} V_{ij}(r_{ij}), \tag{2}$$

TABLE I. Pairwise potential parameters. D and ϵ are in eV. r_0 and σ are in Å. α is in Å^{-1}.

System	D or ϵ	α	r_0 or σ
Xe–Xe	0.024 214 05	1.467 6	4.362 3
Xe–O	0.007 570 2		3.549 39
Xe–N	0.006 809 4		3.742 15
Xe–H	0.002 211 8		3.802 15

where r_{ij} is the distance between the ith and jth lattice atoms, and V_{ij} is a Morse potential with cutoff at $r_{ij}=R_c$, i.e.,

$$V_{ij}=D\{\exp[-2\alpha(r_{ij}-r_0)] - 2\exp[-\alpha(r_{ij}-r_0)]\} \quad \text{for } r_{ij} \leqslant R_c$$
$$V_{ij}=0 \quad \text{for } r_{ij}>R_c. \tag{3}$$

V_i is also taken to have pairwise form,

$$V_i=\sum_{i}^{N}\sum_{k}^{4} V_{ik}(r_{ik}), \tag{4}$$

where V_{ik} gives the interaction between the ith lattice atom and the kth atom of HONO. The V_{ik} term is taken to be a Lennard-Jones(12,6) potential,

$$V_{ik}=\epsilon[(\sigma/r_{ik})^{12}-2(\sigma/r_{ik})^{6}]. \tag{5}$$

When the LJ(12,6) potential is written as shown in Eq. (5), the well depth relative to the energy of the separated atoms is $-\epsilon$ at an equilibrium separation $r_{eq}=\sigma$. A more frequently used definition of the LJ(12,6) potential omits the factor of 2 multiplying the attractive term in Eq. (5) and the factor of ϵ is replaced with 4ϵ. This form can be obtained from Eq. (5) by replacement of σ with $2^{1/6}\sigma$. The two forms are therefore equivalent although the physical interpretation of σ is different for the two cases.

The potential parameters for the various terms are given in Table I. The standard combining rules, arithmetic mean for the equilibrium distance, and the geometric mean for the well depth, have been used together with data previously reported in the literature to obtain the interaction parameters.[8,10,11,18(c)]

The HONO intermolecular potential described in Ref. 13 has been used for V_h. This potential consists of 3 bond stretching terms which are taken as Morse functions, 2 harmonic bending terms, and one cosine series of the dihedral angle to account for torsional effects. The potential uses attenuation terms to smoothly switch between the *cis* and *trans* geometries. It has been shown[13] that this potential yields very good results for the predicted HONO geometry, energetics, and normal-mode frequencies.

III. METHODS AND RESULTS

A. Initial state selection

Intramolecular vibrational energy redistribution rates, internal energy relaxation to phonon modes, and isomerization rates of HONO in xenon are examined using molecular dynamics methods. In all calculations, HONO is initially given 1.7 eV of vibrational energy. Initial rotational energy is set to zero. In addition to zero-point energy in all modes, one or more vibrational modes, as indicated in Table II, are assigned a few quanta of vibrational energy so that the total internal energy is close to 1.7 eV. Vibrational phase averaging is incorporated by a random selection of phase for each normal mode. Subsequently, the vibrational energy is scaled so as to make it exactly 1.7 eV.

TABLE II. Computed *cis*→*trans* isomerization rate coefficients for HONO in the gas phase and under matrix-isolated conditions in Xe at 12 K.

	k (ps^{-1})	
Initial distribution	Xe matrix	Gas phase
(1,2,3,4,5,0)	0.95	0.72
(3,0,0,0,0,0)	0.80	0.23
(0,6,0,0,0,0)	0.53	0.15
(0,0,8,0,0,0)	2.71	2.11
(0,0,0,10,0,0)	0.79	0.27
(0,0,0,0,16,0)	0.59	0.20

The pure xenon lattice is relaxed to its most stable configuration using a damped trajectory method.[11] In this method, the kinetic energy of each lattice atom is set to zero and Hamilton's equations are integrated. When the total kinetic energy of the system passes through a maximum, the integration is halted and the momentum components of the P and Q zone atoms are once again set to zero. This procedure is repeated until the total system energy converges to a minimum. For the pure Xe lattice, we have previously shown[11] that this minimum corresponds closely to the experimental minimum for a xenon crystal at 0 K. The nearest-neighbor Xe–Xe spacing is in near exact accord with the measured result, and the computed sublimation energy of the crystal (4284 cal/mol) is within 13% of the reported value.[11]

Subsequently, the vibrationally-excited HONO molecule is placed inside the matrix such that its center of mass coincides with the center of the innermost unit cell of the (5 ×5×5) lattice. A random rotation of HONO about each of the three primitive translational axes of the fcc crystal is performed to ensure random orientation of HONO within the matrix environment. Finally, the lattice is again relaxed in the field produced by the matrix-isolated HONO molecule using a damped trajectory during which the HONO molecule is held fixed. The final position achieved is taken as the initial configuration of the system. This state generally corresponds to a metastable, local minimum rather than the system global minimum. This is also the case for an experimental system vapor deposited at 12 K without subsequent annealing of the lattice.

The lattice atoms are given momenta determined by the system temperature, T. This is done by assigning each momentum component of each lattice atom a momentum equal to $\pm(2mk_bT)^{1/2}$, where m is the lattice-atom mass and k_b is Boltzmann's constant. The sign of the momentum is chosen randomly.

The effects of energy transfer to the bulk are incorporated using the velocity reset method developed by Riley,

Coltrin, and Diestler.[21] To effect this procedure, the 666 lattice atoms are partitioned into *P*, *Q*, and *B* zones as described in Ref. 10. The velocity reset is applied throughout the trajectory to all *Q*-zone atoms using the reset parameters previously given.[10] During the numerical integration, the boundary atoms (*B*-zone) are held fixed. Consequently, the equilibrium states to which the damped trajectory procedure relaxes the system are states at constant (T,V) rather than states at constant (T,P) as is the case for most matrix experiments. However, we have previously shown[11] that the volume expansion of the local environment produced by matrix isolation of 1,2-difluoroethane decreases rapidly with increasing radial distance and becomes vanishing small beyond a radial distance of 10 Å measured from the center of the innermost unit cell of the lattice. With HONO, the effect will be even smaller. Consequently, the volume change of the crystal produced by the presence of HONO is negligible. Under these conditions, we expect that the equilibrium states and the dynamics of the constant (T,V) matrix model will adequately represent the actual experiment, which is conducted under constant (T,P) conditions.

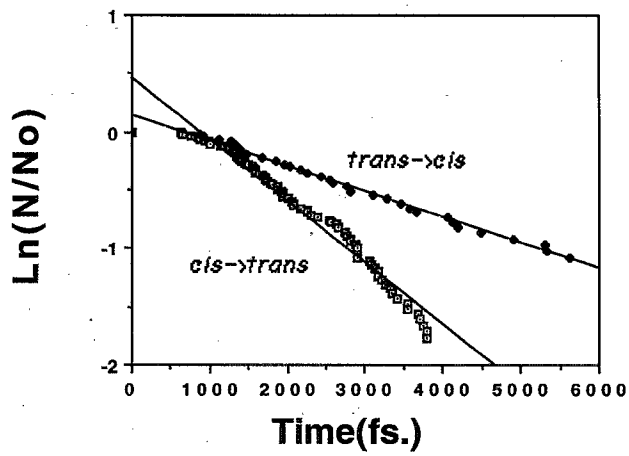

FIG. 1. Logrithmic decay plots for the isomerization reactions of HONO in a Xe matrix at 12 K with 1.7 eV of internal vibrational energy present as zero-point energy and excitation of the N=O stretching mode. The points are results of trajectory calculations. The lines are least squares fits.

B. Isomerization rate coefficients

Isomerization is defined in terms of the HONO dihedral angle, ϕ. The equilibrium *cis* conformation has $\phi=0°$, whereas the *trans* isomer has $\phi=180°$ at equilibrium. $cis \rightarrow trans$ isomerization is defined to have occurred whenever the dihedral angle for a *cis* conformation changes such that ϕ falls in the range $170° \leq \phi \leq 180°$. When this occurs, the reaction time is taken to be the time at the crossing of the barrier crest, which occurs at $\phi=85°$. For $trans \rightarrow cis$ isomerization, reaction is considered to have occurred whenever ϕ is found to lie in the range $0° \leq \phi \leq 10°$. In this case, the reaction time is again taken to be the time of barrier crossing.

Table II gives the calculated $cis \rightarrow trans$ isomerization rate coefficients as a function of the initial energy distribution among the six vibrational modes of HONO. The notation (1,2,3,4,5,0) for the distribution denotes an initial distribution such that in addition to zero-point energy in all modes, we have $n_1=1$, $n_2=2,\ldots,n_6=0$, where the n_i correspond to the number of quanta present of vibrational energy of frequency ν_i. The actual modes correspond to the O–H stretch, N=O stretch, HON bend, O–N stretch, ONO bend, and the torsional mode for $i=1-6$, respectively. In scaling the vibrational energy to 1.7 eV, all modes are scaled proportionately. Table II lists the computed gas phase $cis \rightarrow trans$ isomerization rate coefficients. These results are in good accord with similar calculations previously reported by Guan and Thompson.[16]

The isomerization rate coefficients are obtained from the slope of logarithmic decay plots obtained from the results of 70 to 100 trajectories. Typical results are shown in Fig. 1. Each trajectory is run for a maximum of 1.9 ps except for those sets which are slow. For slow sets, the maximum run time is 3.8 ps.

Table III gives the corresponding results for the $trans \rightarrow cis$ isomerization. These data are obtained by running 50 trajectories for each set for a maximum run time of 5.7 ps for the HONO/Xe system. In the gas-phase, the isomerization process is very slow. Consequently, 100–200 trajectories with a maximum period of 7.7 ps are computed to obtain the decay plots. Figure 1 also shows a typical result for $trans \rightarrow cis$ isomerization.

A superficial consideration of isomerization under matrix-isolated conditions might suggest that steric effects should work to decrease the rate coefficient for such reactions. However, as the data in Tables II and III demonstrate, the opposite effect is observed. In all cases, the isomerization rate is enhanced by the presence of the matrix. The isomerization rate is essentially determined by the intramolecular energy transfer rate between the excited and torsional modes in HONO.[14,16,17] In effect, the coupling terms with the lattice atoms provide an additional pathway for this transfer so that the total transfer rate is the gas-phase mode-to-mode rate plus the mode-lattice rate. The results indicate that this enhancement in the IVR rate to the torsional mode is more important than steric considerations which would tend to decrease the isomerization rate. For the cases considered, the difference in the $cis \rightarrow trans$ isomerization rate,

TABLE III. Computed $trans \rightarrow cis$ isomerization rate coefficients for HONO in the gas phase and under matrix-isolated conditions in Xe at 12 K.

	$k(\text{ps}^{-1})$	
Initial distribution	Xe matrix	Gas phase
(1,2,3,4,5,0)	0.31	0.03
(3,0,0,0,0,0)	0.37	0.006[a]
(0,6,0,0,0,0)	0.22	0.09
(0,0,8,0,0,0)	0.40	0.10
(0,0,0,10,0,0)	0.25	0.11
(0,0,0,0,16,0)	0.35	0.07

[a]Only 9 trajectories out of 200 isomerized in 7.664 ps. The rate is therefore computed directly from the exponential decay equation without plotting the decay curve.

$\Delta k = k_{iso}(\text{matrix}) - k_{iso}(\text{gas})$, varies from 0.23 to 0.60 ps^{-1} with a mean value of 0.45 ps^{-1}. For the *trans→cis* reaction, $\langle \Delta k \rangle = 0.25\ ps^{-1}$.

The data given in Tables II and III show that significant mode specificity is present in the matrix as well as in the gas phase. However, the nature of the mode specificity is altered by the matrix. In the gas phase, excitation of the HON bending mode is 8 times as effective in promoting *cis→trans* isomerization than is the O–N stretch, which is the second most effective mode to excite. The N=O and O–N stretches and the HON bend are nearly equally effective in promoting gas-phase *trans→cis* isomerization. These modes are more than an order of magnitude more effective than the O–H stretch. In the matrix environment, however, the HON bend is the most effective in promoting both isomerizations. Most striking, however, is the increased efficiency of the O–H stretch in promoting the *trans→cis* isomerization. In the matrix, excitation of this mode is almost as effective as the HON bend whereas in the gas-phase, the O–H stretch is almost uncoupled to the torsional motion.

At much lower excitation energies, McDonald and Shirk[19] and Shirk and Shirk[20] found qualitatively similar behavior in their experimental investigations of the isomerization dynamics of matrix-isolated HONO. When the first overtone of the O–H stretching mode is excited, these investigators found that the ratio of the *cis→trans* isomerization to that for *trans→cis*, k_{ct}/k_{tc}, is about 200. If the first N=O stretch overtone is excited, this ratio is greater than 1000. In the present calculations, these ratios are significantly reduced although the same qualitative trends are observed. For excitation of the third O–H overtone, we find $k_{ct}/k_{tc} = 2.16$. If the sixth overtone of the N=O stretch is excited, the result is $k_{ct}/k_{tc} = 2.41$. The 500-fold difference between the calculated and measured[19,20] k_{ct}/k_{tc} ratios is probably not due to the energetic difference between the second and sixth N=O overtones. We have carried out a few calculations for a (0,4,0,0,0,0) initial partitioning. When the fourth N=O overtone is excited, we obtain $k_{ct}/k_{tc} = 1.75$. Thus, we do not approach the results reported by Shirk and co-workers[19,20] at lower excitation energies. Examination of the gas-phase results given in Tables II and III for a (0,6,0,0,0,0) initial partitioning shows that $(k_{ct}/k_{tc})_{gas} = 1.67$. We therefore do not expect the differences between the calculated and measured ratios to be due to lattice imperfections present in the experimental matrix. The discrepancy could be the result of our assumption of classical mechanics or of inaccuracies in the potential-energy surface used in the calculations. It seems unlikely, however, that the combined error due to these effects would be as large as a factor of 500. We therefore suggest that a reexamination of the experimental system is appropriate.

Our previous investigation of statistical/nonstatistical behavior in silene,[22] silane,[23,24] 1,2-difluoroethane,[25–27] and the 2-chloroethyl radical[27] indicate that unimolecular reactions will tend to exhibit statistical behavior whenever the bonding in the fragment or molecule produced by the reaction is significantly altered from that present in the original molecule. Since the bonding in *cis*- and *trans*-HONO is nearly identical, we would predict that nonstatistical dynamics should be present. As the data in Tables II and III demonstrate, this is the case. Our previous studies[26] have also shown that such nonstatistical dynamics often persist at energies well in excess of threshold. For example, C–H and C–F bond fission reactions of 1,2-difluoroethane are nonstatistical even at energies 5.0 eV in excess of the dissociation threshold.[26] The nonstatistical dynamics observed in the present study for *cis–trans* isomerization reactions of HONO at 1.7 eV are another example since this energy is about 1.3 eV greater than the isomerization barrier.

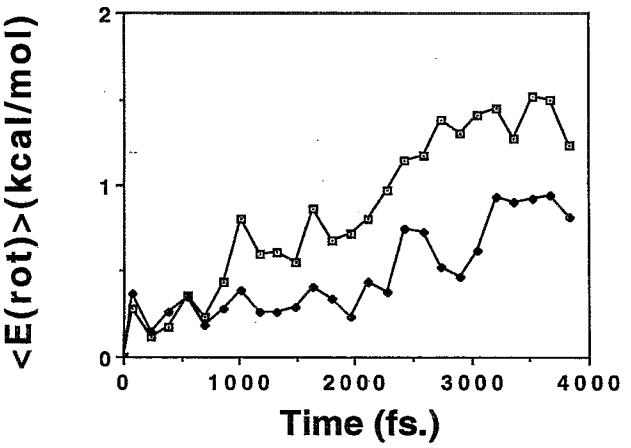

FIG. 2. Average rotational energy of HONO in kcal/mol as a function of time in femtoseconds. Open rectangles correspond to the average over isomerized trajectories. Solid rectangles represent the results from nonreactive trajectories. The initial energy is partitioned into the N=O stretch with the assignments (0,6,0,0,0,0).

The interaction of HONO with the lattice is seen to impart a significant amount of rotational energy to HONO. Figure 2 shows a typical result. This type of energy transfer has also been observed for 1,2-difluroethane isolated in Ar, Kr, and Xe matrices. In this case, the effect was termed "rotational reorientation."[11] Guan and Thompson[16] have previously shown that the presence of rotational angular momentum enhances the energy transfer to the torsional mode of HONO and hence the rate of isomerization. The data given in Fig. 2 demonstrate that this effect is also present in the matrix-isolated system. The upper curve in Fig. 2 includes only those trajectories which undergo isomerization while the lower curve includes those trajectories which do not isomerize during the time period examined in the trajectories. The correlation between HONO rotation and energy transfer to the torsional mode is obvious. Consequently, it seems likely that the additional energy transfer pathway opened by the presence of the matrix involves a (vibration→lattice phonon modes→rotation→torsional vibration) mechanism.

C. Effect of lattice defects

In many experiments, the lattice is not perfect. Depending on the deposition conditions, the number density of lattice atoms may be only 80%–90% that of the corresponding

TABLE IV. Computed *cis→trans* isomerization rate coefficients for HONO as a function of the percentage vacancies in the Xe lattice at 12 K for a (0,6,0,0,0,0) initial energy partitioning.

% Vacancies	$k(ps^{-1})$
0	0.53
10	0.25
20	0.16
100 (gas phase)	0.15

perfect fcc lattice.[9] To simulate such lattice defects, we have carried out two sets of computations. In the first set, 65 randomly chosen lattice atoms are removed. Subsequent to this removal, the lattice is relaxed to its new local minimum potential energy. This process is repeated for each trajectory to properly average over the local environments for the trapped HONO molecules. The remainder of the procedure is as described for the fcc lattice. In the second set, 130 atoms are randomly removed.

Table IV gives the rate of *cis→trans* isomerization for Xe lattices with 10% and 20% vacancies. For comparison, the corresponding data for the perfect lattice and the gas phase are also reported. As the number of vacancies increases, the matrix-induced enhancement of the isomerization decreases. When 130 lattice atoms (≈20%) are removed, the isomerization rate is seen to approach the gas-phase rate. Thus, it appears that a lattice with about 20% vacant sites can isolate a molecule such as HONO with little perturbation on its gas-phase behavior. Similar results have previously been obtained for F_2/C_2H_4 pairs in Xe matrices.[9] In the gas phase, F_2 adds to ethylene via an atomic addition mechanism in which the major products are $H_2C{-}CH_2F{+}F$.[28] In contrast, when isolated in a perfect fcc Xe matrix, atomic addition plays only a minor role.[10] The principal mode of reaction involves an $\alpha\beta$-addition across the ethylene double bond. This addition results either in a stabilized 1,2-difluroethane molecule after energy transfer to the phonon modes or HF elimination to form $H_2C{=}CHF{+}HF$.[10] If, however, a simulated vapor-deposited matrix containing approximately 20% vacancies is employed in the calculations, the major reaction mechanism is found to be atomic addition.[9] Consequently, the present calculations combined with those obtained for the F_2/C_2H_2/Xe system[9,10] indicate that gas-phase behavior will be approached as the number of Xe lattice vacancies approaches 20%.

D. Vibrational relaxation to phonon modes

The coupling between HONO and the lattice atoms produces a characteristic energy transfer rate to the phonon modes of the lattice. This rate can often be accurately represented by a first-order rate law,

$$dE_v/dt = -k_v(E_v - E_{eq}). \tag{6}$$

In Eq. (6), E_v is the vibrational energy of HONO, E_{eq} is the value of E_v when HONO is in thermal equilibrium with the lattice at temperature T, and k_v is the characteristic energy transfer rate coefficient. In the present study, we generally have $E_{eq} \ll E_v$ so that the slope of a logarithmic plot of E_v as a function of time is $-k_v$.

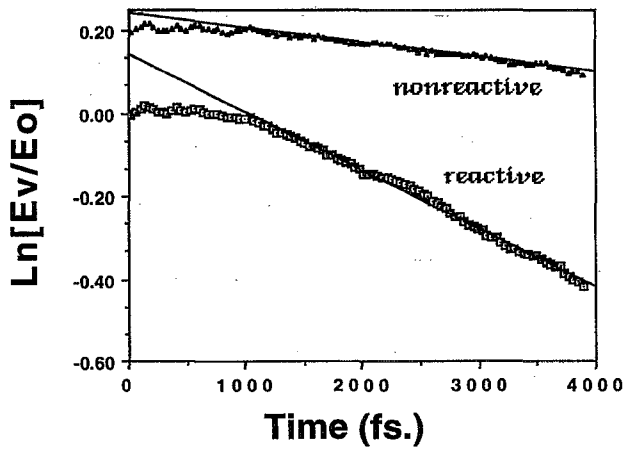

FIG. 3. Log of the ratio of the average HONO vibrational energy to its initial value as a function of time. The open rectangles represent that data for the isomerized trajectories. The solid triangles denote the data for unisomerized trajectories. The straight lines are least-squares fits. The initial energy partitioning is (0,6,0,0,0,0). For visual clarity, the ordinate value for the unisomerized trajectories is increased by 0.2 at all points.

Figure 3 shows a typical decay plot for E_v. The upper and lower curves are the results for nonreactive and reactive trajectories, respectively. The rate coefficients extracted from the slopes of such decay plots are reported in Table V for different initial partitionings of the 1.7 eV of vibrational energy. As can be seen, the relaxation rate to phonon modes of the lattice is significantly greater for trajectories undergoing isomerization than for the ensemble of nonreactive trajectories. Since energy transfer to the lattice enhances isomerization via the mechanism (vibration→lattice phonon mode→rotation→torsional vibration), this is the expected result.

The relationship between isomerization and energy transfer to the lattice may be clearly seen by following the time variation of the HONO dihedral angle and the HONO internal energy for both reactive and nonreactive trajectories. Figures 4 and 5 show such cases. The trajectory shown in Fig. 4 undergoes *cis–trans* isomerization at approximately 600 fs. Simultaneously, the internal energy in HONO begins

TABLE V. Rate coefficients for energy transfer to the Xe lattice phonon modes at 12 K as a function of initial HONO energy distribution and the percentage of vacancies in the lattice.

		k_v (ps^{-1})	
Initial distribution	% Vacancies	Isomerized	Unisomerized
(1,2,3,4,5,0)	0	0.17	0.043
(0,0,8,0,0,0)	0	0.18	0.041
(0,6,0,0,0,0)	0	0.14	0.035
(0,6,0,0,0,0)	10	0.04	0.005
(0,6,0,0,0,0)	20	0.03	0.004

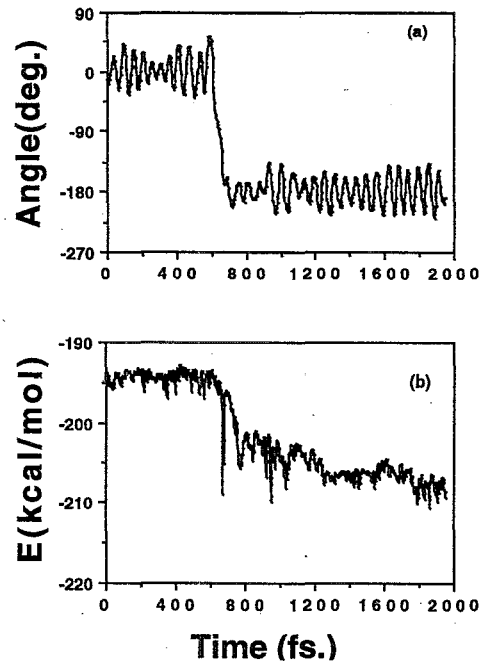

FIG. 4. (a) The variation of the HONO dihedral angle as a function of time for a trajectory undergoing *cis→trans* isomerization. The initial energy partitioning is (0,6,0,0,0,0). (b) The corresponding variation of HONO internal energy in kcal/mol. The energy zero corresponds to the energy of totally dissociated HONO with all atoms at rest.

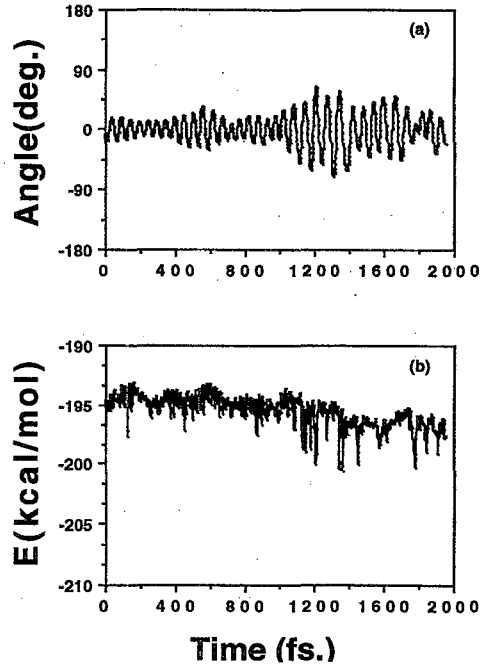

FIG. 5. Same as Fig. 4 for a nonreactive trajectory.

to rapidly decrease. There is obviously a large coupling between the lattice phonon modes and the HONO torsional mode. In contrast, the nonreactive trajectory shown in Fig. 5 exhibits no such rapid decrease in the HONO internal energy.

The data in Table V also show that the energy transfer rate to the lattice phonon modes decreases as the number of lattice vacancies increases. With 20% vacancies, the calculated decrease is a factor of 4.6. This is very similar to the result for 1,2-difluoroethane where it has been found that the energy transfer rate to the lattice decreases by about a factor of 4 when a perfect fcc lattice is replaced by one having about 18% vacancies.[9]

It is interesting to note that very little mode specificity is seen for energy transfer to lattice phonon modes. For example, we find that $k_v(0,0,8,0,0,0)/k_v(0,6,0,0,0,0)$ is 1.29. This difference is not much greater than the statistical uncertainty in the calculations. It may be that the HONO→lattice energy transfer rate is near its maximum or saturated value for each initial partitioning investigated. The Debye frequency of the present model lattice is 0.62 ps^{-1}. If a few vibrations of the lattice atoms are required to remove excess energy from HONO, the calculated energy transfer rate coefficient would be significantly less than 0.62 ps^{-1}. The maximum transfer rate computed for HONO is 0.18 ps^{-1}. Consequently, this may well be the saturation value. Additional studies will be required to confirm this concept of a limiting or saturation value for the vibrational relaxation rate to the lattice phonon modes.

E. Intramolecular energy transfer

The *cis–trans* isomerization rates and the statistical/nonstatistical behavior of the system are critically dependent upon the IVR rates. If the IVR rates are globally rapid compared to the unimolecular reaction rate, statistical dynamics are expected but not otherwise.

Figures 6 and 7 show the time variation of the energy in each of the 6 vibrational modes of HONO for gas-phase and matrix-isolated systems, respectively, for a (0,6,0,0,0,0) initial partitioning into the N=O stretch. The "instantaneous" local-mode energies are taken to be twice the average local-mode potential where this average is computed over 156 fs. Each point in the plots shown in Figs. 6 and 7 represents the average over all trajectories in the set. An inspection of Fig. 6 immediately shows that IVR is not globally rapid in the gas phase. The average energy in the HON bend remains nearly constant throughout the process. Table II shows that the isomerization rate for this initial partitioning is 0.15 ps^{-1} in the gas phase. This corresponds to a halflife of 4600 fs. Inspection of the internal N=O energy given in Fig. 6 shows that at 4600 fs less than half of the initial N=O mode energy has been transferred. Consequently, it is clear that the isomerization rate exceeds the IVR rate in the gas-phase. Under such conditions, we expect the dynamics to be nonstatistical.

The same analysis may be carried out for matrix-isolated HONO. Here, the isomerization rate from Table II is 0.53 ps^{-1} which corresponds to a halflife of 1300 fs. The data given in Fig. 7 shows the halflife for N=O relaxation to be significantly greater than 1300 fs. Consequently, isomeriza-

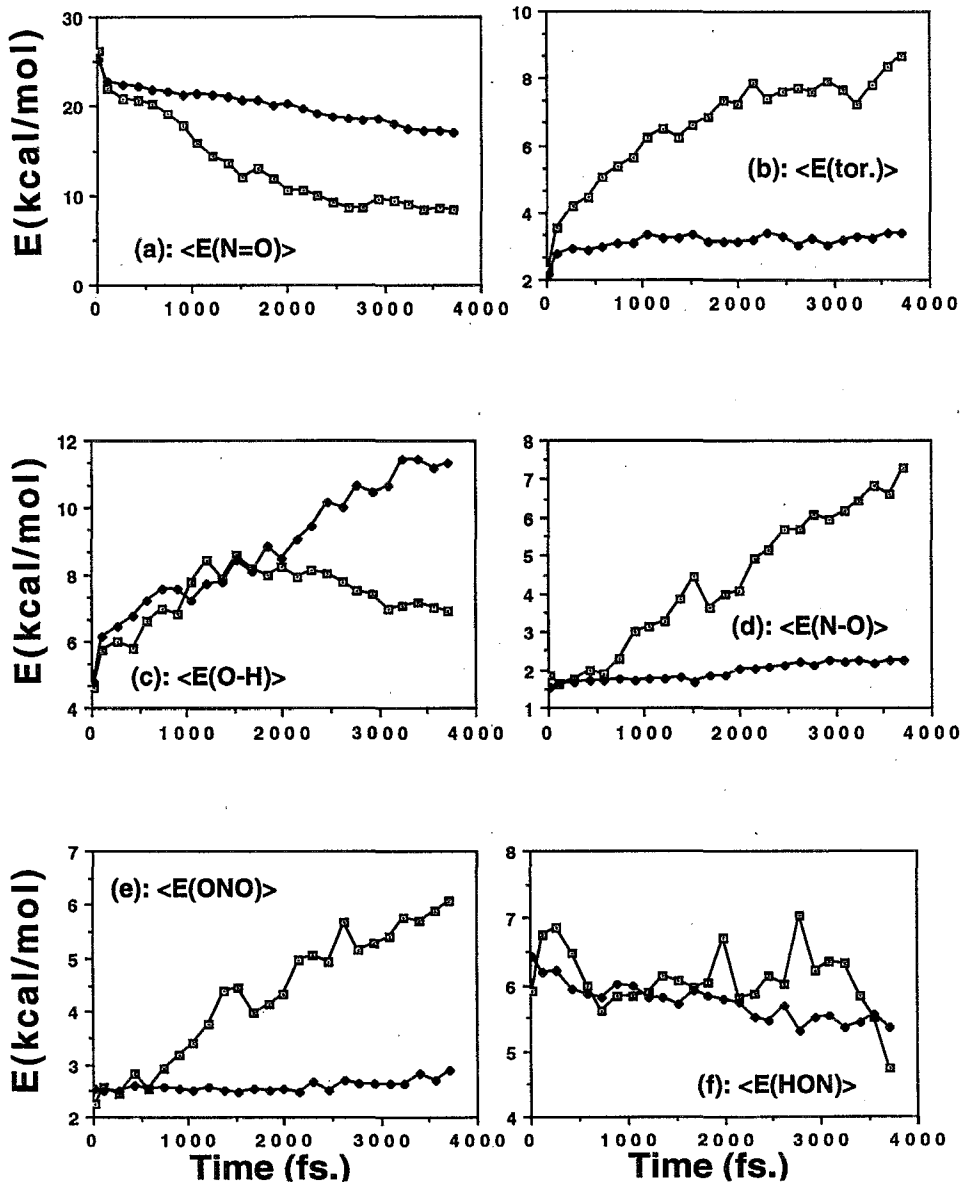

FIG. 6. Average HONO energy in different local modes in kcal/mol as a function of time in femtoseconds for gas-phase reactions of HONO. The open rectangles correspond to the average over isomerized trajectories. The solid rectangles represent unisomerized trajectories. The initial *cis*-HONO energy partitioning is (0,6,0,0,0,0). (a) N=O stretch; (b) torsional mode; (c) O–H stretch; (d) N–O stretch; (e) ONO bending mode; (f) HON bending mode.

tion is faster than IVR in the matrix as well as in the gas phase. Therefore, the nonstatistical dynamics which our previously formulated generalization predicts[27] are in accord with the calculated IVR rates as well as with the observed mode specificity of the reaction.

The effect of energy transfer to the lattice phonon modes may be seen by a comparison of Figs. 6 and 7. In the gas phase (Fig. 6), we note that there is a sharp difference between the energy gained by the N–O stretch, the ONO bend, and the torsional modes for reactive and nonreactive trajectories. In the matrix (Fig. 7), however, the magnitude of these differences are sharply reduced due to HONO-lattice coupling. Stated in another way, the lattice phonon modes provide a pathway that couples the N=O stretch more effectively with the N–O stretch, the ONO bend, and the torsional modes.

A comparison of the torsional energy variation in the matrix and the gas phase leads to an interesting inference. As noted above, the difference in energy transfer to the torsional modes between reactive and unreactive trajectories is much less in the matrix than in the gas phase. Consequently, it is reasonable to infer that in the matrix, the nonreactive trajectories are, on average, much closer to the isomerization threshold than is the case in the gas phase. This suggests that the isomerization rate of HONO in the matrix is much more sensitive to small variations in the barrier height, initial energy, etc. A more detailed study is required to confirm this inference. However, if true, this suggests that dynamical data

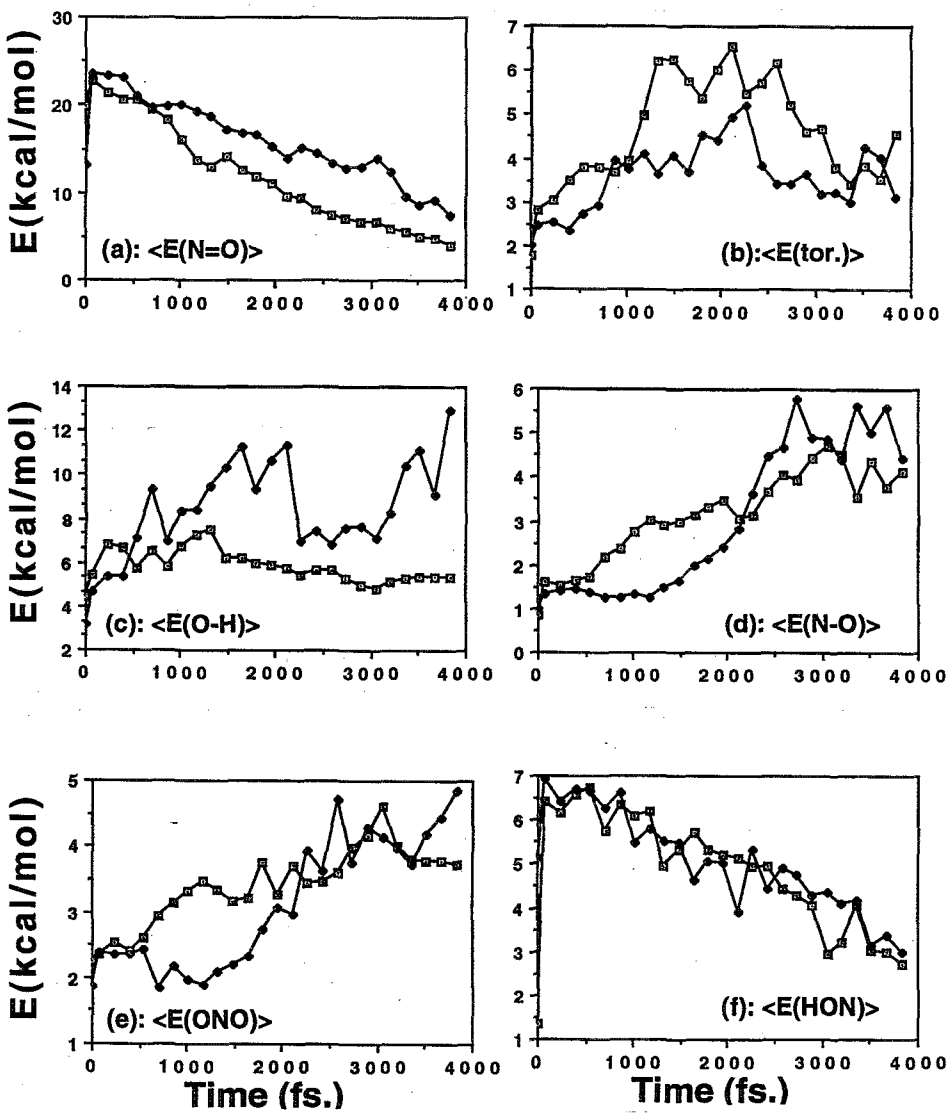

FIG. 7. Same as Fig. 6 except that HONO is matrix isolated in a fcc xenon lattice.

obtained under matrix-isolation conditions are more sensitive probes than the corresponding gas phase data.

The energy variation patterns for HONO in an imperfect lattice with vacancies is expected to be intermediate to the two limiting cases. This is the observed result. For example, we find that the rotational energy gain by HONO increases as the number of vacant sites decreases. We also find that the difference between the torsional energy of isomerized and unisomerized trajectories decreases as the number of vacant sites decreases.

IV. SUMMARY

Theoretical molecular dynamics studies of *cis–trans* isomerization, intramolecular vibration relaxation (IVR), and vibrational relaxation rates to lattice phonon modes of HONO isolated in a face-centered cubic xenon matrix at 12 K have been reported. The effect of the matrix environment upon the dynamics has been obtained by comparison with the corresponding gas-phase results. Questions related to statistical vs nonstatistical behavior and the effect of lattice imperfections have been addressed.

It is found that both *cis*→*trans* and *trans*→*cis* isomerization rates are significantly enhanced by the presence of the matrix in spite of the steric effects produced by the environment. Comparison of the rate coefficients for different initial energy partitioning suggests that this result occurs because the matrix opens an additional energy transfer pathway to the torsional mode that is best described as a (vibration→lattice phonon mode→rotation→torsional vibration) mechanism. The presence of this pathway is confirmed by calculations that show that HONO rotation is highly coupled to the phonon modes of the lattice and to the torsional mode of HONO.

The calculated isomerization rate coefficients show the

presence of significant nonstatistical dynamics. This observation confirms the prediction that reactions which produce little or no change in the bonding in the products should exhibit nonstatistical behavior.[27] We also find that the IVR rates in the matrix and in the gas phase are slow relative to the isomerization rates. Consequently, the reactions cannot be statistical. The calculated ratio for $cis \rightarrow trans$ and $trans \rightarrow cis$ isomerization, k_{ct}/k_{tc}, is larger for excitation of the N=O stretch than is the case when an equal amount of energy is initially partitioned into the O–H stretch. This is in qualitative agreement with previously reported measurements by Shirk and co-workers.[19,20] However, the calculated k_{ct}/k_{tc} ratio is about a factor of 500 less than the measured value.[19,20] This discrepancy does not appear to be due to a difference in total excitation energy nor to the presence of lattice defects in the experimental matrix. It could be a result of our assumption of classical mechanics or to inaccuracies in the potential-energy surface. In view of the magnitude of the discrepancy, a re-examination of the experimental system seems warranted.

Vibrational relaxation to the lattice phonon modes are found to be almost independent of the initial energy partitioning. It is suggested that this may be a result of "saturation." That is, the HONO-lattice transfer rates may be approaching their limiting values determined by the Debye frequency of the lattice.

The presence of lattice vacancies is found to exert a profound influence upon the dynamics. When the percentage of lattice vacancies approaches 20%, the calculated dynamics in the matrix are found to approach the gas-phase behavior. This result is in good accord with similar data previously obtained for F_2/C_2H_4 pairs isolated in Ar, Kr, or Xe matrices.[9]

ACKNOWLEDGMENTS

We are pleased to acknowledge financial support from the National Science Foundation Grant No. CHE-9211925 and from the Air Force Office of Scientific Research Grant No. F49620-92-J-0011. P. M. A. thanks Vikram University, Ujjain, India, for granting him leave to pursue this research.

[1] E. Whittle, D. A. Dows, and G. C. Pimentel, J. Chem. Phys. **22**, 1943 (1954).
[2] *Chemistry and Physics of Matrix-Isolated Species*, edited by L. Andrews and M. Moskovitis (North–Holland, Amsterdam, 1989).
[3] *Cryochemistry*, edited by M. Moskovits and G. A. Ozin (Wiley–Interscience, New York, 1976).
[4] A. I. Krylov and R. B. Gerber, J. Chem. Phys. **100**, 4242 (1994).
[5] C. Lugez, A. Schriver, R. Levant, and L. Schriver-Mazzuoli, Chem. Phys. **181**, 129 (1994).
[6] J. Wolf and G. Hohlneicher, Chem. Phys. **181**, 185 (1994).
[7] R. Fraenkel and Y. Haas, Chem. Phys. Lett. **220**, 77 (1994).
[8] M. B. Ford, A. D. Foxworthy, G. J. Mains, and L. M. Raff, J. Phys. Chem. **97**, 12 134 (1993).
[9] L. M. Raff, J. Chem. Phys. **97**, 7459 (1992).
[10] L. M. Raff, J. Chem. Phys. **95**, 8901 (1991).
[11] L. M. Raff, J. Chem. Phys. **93**, 3160 (1990).
[12] Y. Qin and D. L. Thompson, J. Chem. Phys. **100**, 6445 (1994).
[13] C. C. Chambers and D. L. Thompson, Chem. Phys. Lett. **218**, 166 (1994).
[14] Y. Qin and D. L. Thompson, J. Chem. Phys. **96**, 1992 (1992).
[15] D. L. Thompson, in *Proceedings of the 24th Jerusalem Symposium on Quantum Chemistry, Mode Selective Chemistry*, edited by B. Pullman, J. Jortner, and R. D. Levine (Reidel, Dordrecht, 1991), p. 261.
[16] Y. Guan and D. L. Thompson, Chem. Phys. **139**, 147 (1989).
[17] Y. Guan, G. C. Lynch, and D. L. Thompson, J. Chem. Phys. **87**, 6957 (1987).
[18] (a) R. T. Hall and G. C. Pimentel, J. Chem. Phys. **38**, 1889 (1963); (b) J. D. Baldeschwieler and G. C. Pimentel, *ibid.* **33**, 1008 (1960); (c) R. Gunde, P. Felder, and Hs. H. Gunthard, Chem. Phys. **64**, 313 (1982).
[19] P. A. McDonald and J. S. Shirk, J. Chem. Phys. **77**, 2355 (1982).
[20] A. E. Shirk and J. S. Shirk, Chem. Phys. Lett. **97**, 549 (1983).
[21] M. E. Riley, M. E. Coltrin, and D. J. Diestler, J. Chem. Phys. **88**, 5934 (1988).
[22] P. M. Agrawal, D. L. Thompson, and L. M. Raff, J. Chem. Phys. **89**, 741 (1988).
[23] (a) P. M. Agrawal, D. L. Thompson, and L. M. Raff, J. Chem. Phys. **92**, 1069 (1990); (b) H. W. Schranz, L. M. Raff, and D. L. Thompson, *ibid.* **95**, 106 (1991).
[24] H. W. Schranz, L. M. Raff, and D. L. Thompson, J. Chem. Phys. **94**, 4219 (1991).
[25] L. M. Raff, J. Chem. Phys. **90**, 6313 (1989).
[26] H. W. Schranz, L. M. Raff, and D. L. Thompson, Chem. Phys. Lett. **182**, 455 (1991).
[27] (a) T. D. Sewell, H. W. Schranz, D. L. Thompson, and L. M. Raff, J. Chem. Phys. **95**, 8089 (1991); (b) X. Y. Chang, T. D. Sewell, L. M. Raff, and D. L. Thompson, *ibid.* **97**, 7354 (1992).
[28] L. M. Raff, J. Phys. Chem. **92**, 141 (1988).